Contributed Paper to Topic B2

FISSION CROSS-SECTION AND RESONANCE PARAMETERS OF ^{241}Am

B. Lucas, H. Derrien and D. Paya
Nuclear Physics Department,
Saclay Nuclear Research Centre,
Gif-sur-Yvette, France

ABSTRACT

The total cross-section of ^{241}Am has provided resonance parameters up to 150 eV. The fission cross-section was measured by means of a fast neutron detector. It provides the fission widths up to 40 eV. The results are compared with those based on measurements made at other laboratories.

Measurement of the fission cross-section of ^{241}Am was performed in order to find a possible intermediate structure similar to the one present in ^{237}Np and several other nuclei. Since previous measurement [1] had not shown a marked effect of this type, however, it was expected that a close analysis of the resonance parameters would have to be made. Furthermore, these resonances, despite their value in calculating reactors, were either well known in only a few cases or else not properly known. For this reason we attempted to measure, successively, the total cross-section and the fission cross-section of ^{241}Am, using the neutron spectrometer installed in the AL60 accelerator at Saclay.

The total cross-section was measured between 0.8 eV and 1 keV. The experimental conditions were described at the previous Kiev conference [2], during which some preliminary results were presented. The analysis has now been completely finished [3]. Table 1 shows for all the resonances identified between 0 and 150 eV the following: energy E, neutron width $2\,g\,\Gamma_n$; statistical error $\Delta(2\,g\Gamma_n)_1$ and error due to background $\Delta(2\,g\Gamma_n)_2$. Moreover, whenever it was possible, the radiative widths Γ_γ were calculated by the difference $\Gamma_\gamma = \Gamma - 2\,g\Gamma_n$ on the assumption that Γ_n and Γ_f are sufficiently small for the approximation introduced by this relationship to be better than the experimental accuracy. The values of Γ_γ as well as the statistical error $\Delta\Gamma_\gamma$ also appear in Table I. Monte Carlo calculations aimed at reproducing a cross-section similar to the one measured show that $(18 \pm 4)\%$ of the levels are not observed in the experimental cross-section. Approximately 80% of these levels are lost because they have a neutron width less than one tenth of the mean width. If we take these lost resonances into account, the true mean spacing is $\langle D \rangle = (0.55 \pm 0.05)$ eV.

Measurement of the fission cross-section made it necessary to develop a new type of detector. Indeed, the strong alpha activity of ^{241}Am considerably reduces the amount of this element that can be put into an ionization chamber or a gas scintillator. Given the poor cross-section and the flux available to us, we had to use a sample of a few grams of americium. We therefore selected a proton recoil detector responsive to fission neutrons and insensitive to resonance neutrons and alpha particles. This detector consists of a truncated cylinder holding 45 litres of NE 213 scintilating liquid and divided into four optically independent parts. Each part is viewed by an XP 1040 photomultiplier. A tube runs along the detector axis, enabling the americium sample to be placed at the centre and permitting the incident neutron beam to pass through. A set of lead and boron screens reduce the gamma radiation and delayed neutron exchange between the liquid and samples. A pulse shape discriminator system cuts out the signals due to gamma radiation at a rejection rate of 10^5 for an 800 keV threshold neutron energy. Preliminary experiments have been made with a sample of 1.5 g of americium oxide. Unfortunately, the reactions (α,n) in the oxide create a fast neutron background that can only be eliminated by imposing coincidences between two diametrically opposite parts of the detector, the disadvantage of which is that the efficiency is greatly reduced. Under the experimental conditions described in Table II, the count rate was 10 fissions per hour at the resonance peak 5.4 eV.

The cross-section was normalized to the Bowman cross-section [4] between 0 and 15 eV. Table III shows the fission widths obtained for 38 resonances below 40 eV. They were calculated on the basis of the parameters in Table I. Matching with the Bowman value is satisfactory for seven of the resonances and poor for four others. In the case of resonances at 3.97, 4.97, 6.12 and 9.11 eV, Bowman gives resonance surfaces some ten times weaker than ours, although there was no apparent disagreement in the cross-sections. The fission widths have a mean value $\Gamma_f = 0.23$ MeV with a χ^2 distribution with 4 degress of freedom (Fig. 1). Hence, there is a fairly large number of channels contributing to the fission below the threshold for the ^{242}Am compound nucleus; this is in fact not impossible when we think that in an uneven-uneven nucleus of this kind the transition states should be very close together.

The results in Table I have also made it possible to analyse the fission cross-section measured at Los Alamos [1](obtained through the Neutron Data Compilation Centre (CCDN) at Saclay). The fission widths obtained between 22 and 52 eV are given in Table IV. Their mean value is $\langle \Gamma_f \rangle = 0.52$ meV and has a χ^2 distribution with 15 degrees of freedom. It is difficult to interpret this result within the theory of fission channels. An explanation might be found in contamination of the fission cross-section by capture. It only needs a 0.7%

contribution to fission by the total capture in order to raise the mean width from 0.23 meV to 0.52 meV. If we apply the corresponding correction of 0.30 meV at each fission width, the number of degrees of freedom drops from 15 to 3 (Fig. 2).

In view of the above remarks, neither our results, nor those of Los Alamos, show anomalies in the distribution of widths suggesting an intermediate structure effect, or at least not below 50 eV. At higher energies, there is nothing to be seen from visual examination of the cross-section, and the statistics obtained in this initial experiment are too poor to permit analysis in terms of resonance parameters.

It should be stressed, however, that although this experiment has enabled us to measure a certain number of fission widths, its aim was basically to verify, under particularly stringent experimental conditions, the capabilities of the fission neutron detector. Since the latter justified the hopes that had been based on it, it would be interesting to remake the measurement, using a sample of americium metal enclosed in a box made of a material with a high atomic number. The detector, then rid of neutrons produced by reactions (α,n), would be able to operate without coincidences. The resulting gain in the detection efficiency would thereby make it possible to work with longer flight distances and to expand the energy analysis region.

REFERENCES

[1] P.A. Seeger et al. Nucl. Phys. A 96 (1967), 605.

[2] H. Derrien. 2nd National Soviet Conf. Kiev (1973), vol.2, p. 246.

[3] H. Derrien et B. Lucas. Conf. on Nucl. Cross Section and Technology, Washington (1975).

[4] C.D. Bowman et al. Phys. Rev. 137 B (1965) 326.

CAPTIONS TO FIGURES

Fig. 1 Number of resonance for which $\sqrt{\Gamma_f}$ is higher than the value given on the abscissa (this experiment).

Fig. 2 Number of resonances for which $\sqrt{\Gamma_f}$ is higher than the value given on the abscissa: (a) analysis of data from Ref. [1]; (b) previous results after subtraction of 0.30 meV.

CAPTIONS TO TABLES

Table I: Resonance parameters for ^{241}Am;

Table II: Experimental conditions for measuring the fission cross-section;

Table III: Fission widths for ^{241}Am;

Table IV: Fission widths derived from data given in Ref. [1].

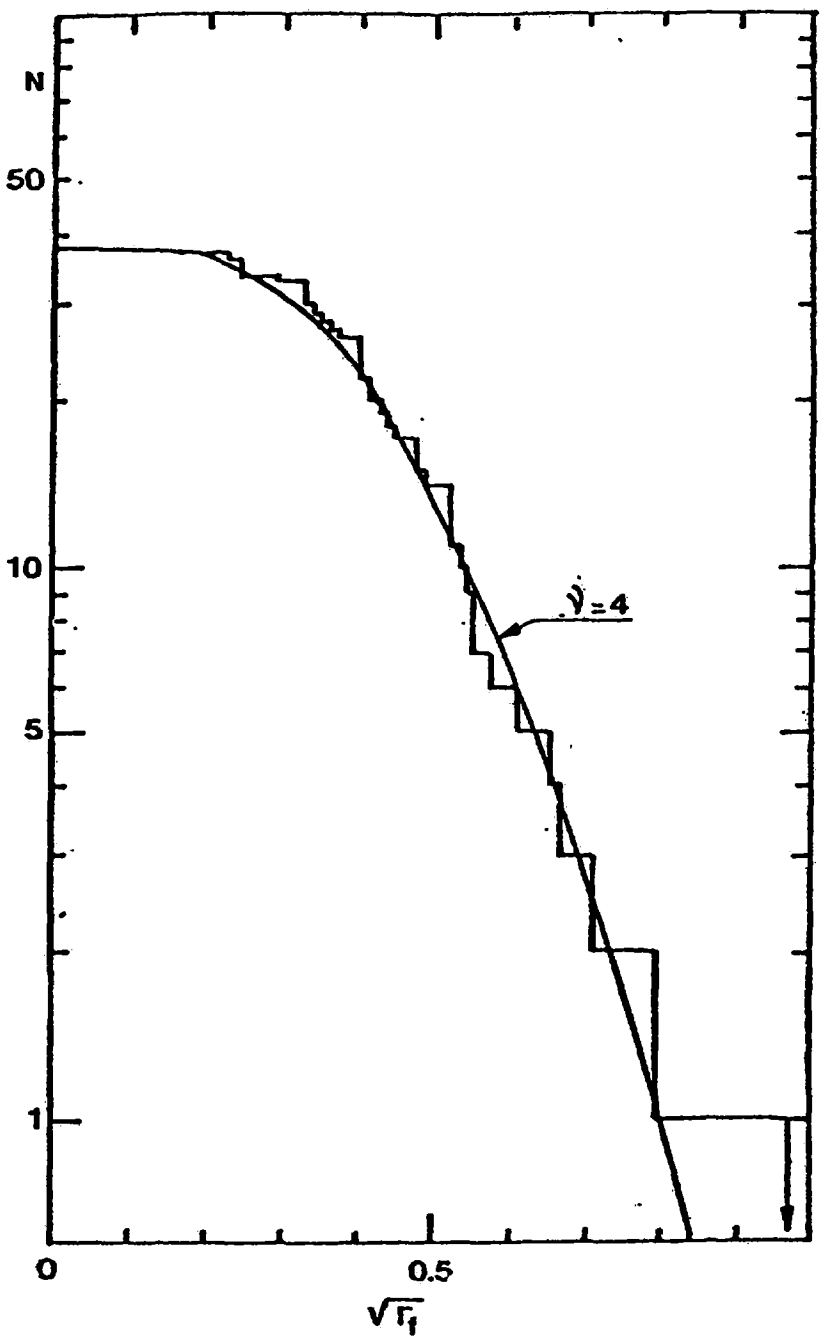

Fig.:1

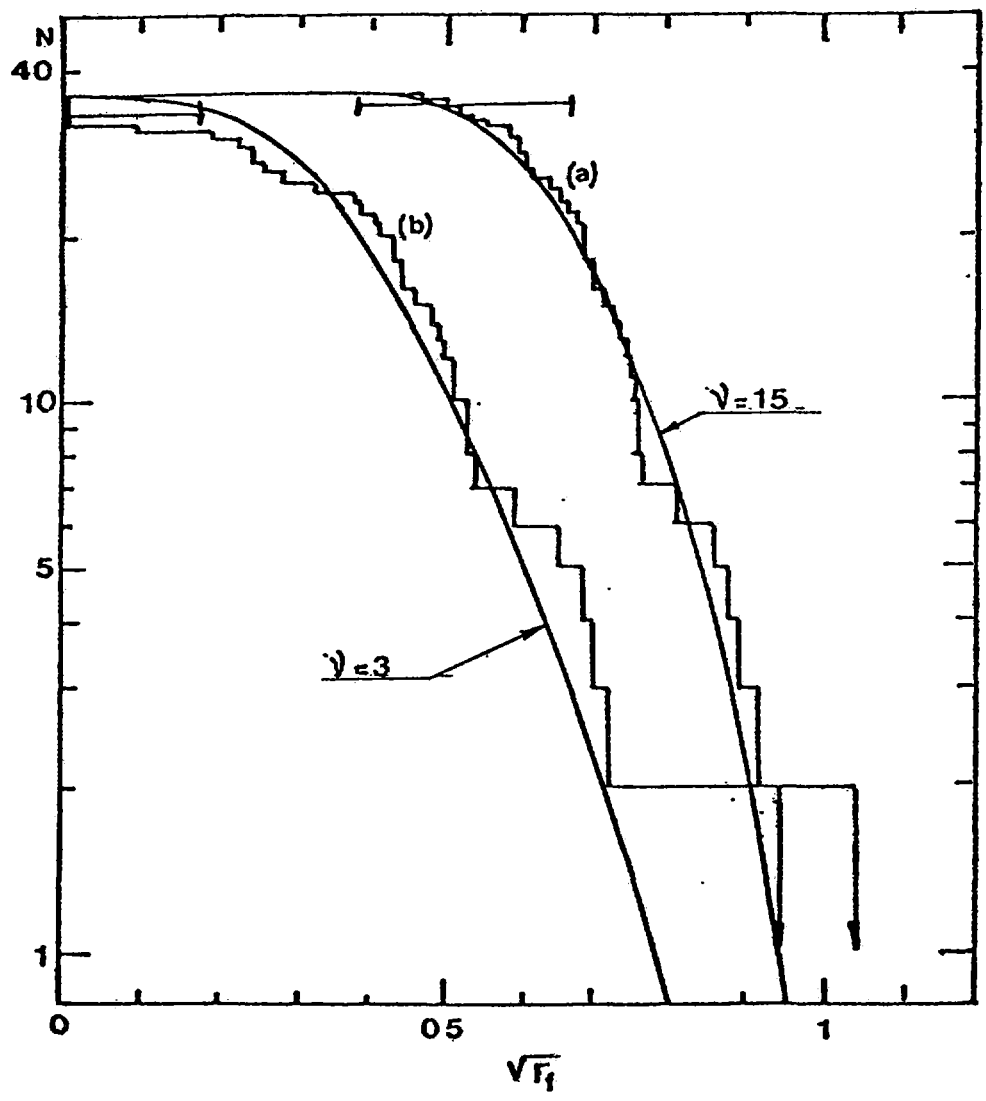

Fig.:2

Table I

E (eV)	$2g\Gamma_n$ (meV)	$\Delta(2g\Gamma_n)_1$ (meV)	$\Delta(2g\Gamma_n)_2$ (meV)	Γ_γ (meV)	$\Delta\Gamma_\gamma$ (meV)	E (eV)	$2g\Gamma_n$ (meV)	$\Delta(2g\Gamma_n)_1$ (meV)	$\Delta(2g\Gamma_n)_2$ (meV)	Γ_γ (meV)	$\Delta\Gamma_\gamma$ (meV)
1.276	0.322	0.006	0.026	46.5	0.8	31.020	0.336	0.010	0.004		
1.928	0.113	0.001	0.006	44.3	0.3	31.251	0.996	0.019	0.015	42.6	4.2
2.372	0.073	0.001	0.004	42.4	0.3	32.030	0.300	0.010	0.003	47.4	8.6
2.598	0.147	0.001	0.010	46.0	0.3	33.510	0.060				
3.973	0.210	0.001	0.006	44.5	0.3	34.028	0.628	0.012	0.008	45.4	4.9
4.968	0.175	0.001	0.004	43.8	0.4	34.460	0.125	0.007			
5.415	0.760	0.003	0.019	44.2	0.1	34.928	0.612	0.012	0.006	42.8	5.4
5.800	0.002					35.485	0.427	0.012	0.004	50.6	8.1
6.117	0.124	0.001	0.002	43.8	0.7	36.250	0.167	0.007	0.001		
6.745	0.028	0.001				36.483	0.100				
7.659	0.037	0.001				36.979	2.995	0.017	0.075	52.0	1.5
8.173	0.108	0.001	0.001	42.7	1.2	38.366	2.260	0.015	0.044	47.0	2.0
9.113	0.389	0.002	0.009	44.2	0.6	38.830	0.055				
9.851	0.406	0.002	0.009	43.9	0.6	39.617	1.295	0.020	0.020	40.2	4.2
10.116	0.026	0.001				40.067	0.541	0.040	0.005	77.9	20.1
10.403	0.326	0.002	0.005	42.4	0.8	40.396	0.948	0.034	0.012	66.0	8.6
10.997	0.413	0.002	0.006	46.5	0.8	41.298	0.084				
11.583	0.016	0.001				41.791	0.355	0.009	0.003		
12.137	0.007	0.001				42.130	0.150	0.009	0.001		
12.879	0.131	0.001	0.001			43.294	0.605	0.033	0.010	18.0	8.9
13.874	0.012	0.001				43.574	0.582	0.035	0.006	36.2	13.6
14.360	0.071	0.002	0.001			44.416	0.118	0.009			
14.682	2.482	0.011	0.075	40.3	0.5	44.921	0.074	0.009			
15.689	0.244	0.003	0.003	39.3	2.9	46.073	0.665	0.018	0.007	43.8	8.6
16.388	1.277	0.005	0.034	41.8	0.9	46.566	0.371	0.018	0.003	22.8	14.0
16.849	0.646	0.004	0.012	41.2	1.5	47.535	1.053	0.017	0.012	41.6	5.2
17.729	0.391	0.004	0.006	37.3	2.4	48.765	0.713	0.018	0.007	40.0	8.0
18.167	0.017					49.332	0.220	0.011	0.002		
19.445	0.213	0.003	0.002			50.278	2.442	0.022	0.042	51.8	3.0
20.333	0.034					50.847	0.393	0.020	0.003	35.8	16.4
20.880	0.089	0.001				51.984	1.385	0.021	0.017	50.2	4.9
21.740	0.081	0.003				53.014	0.165	0.012	0.001		
22.748	0.069	0.003				53.493	0.184	0.012	0.001		
23.079	0.417	0.012	0.005	42.2	6.0	54.407	0.073	0.012			
23.337	0.445	0.012	0.006	42.5	5.8	54.990	1.443	0.025	0.002	108.5	6.9
24.192	1.304	0.007	0.028	39.2	1.5	55.595	0.213	0.014	0.002		
25.008	0.014	0.001	0.001			55.945	1.432	0.034	0.018		
25.634	1.258	0.008	0.025	37.6	1.7	56.158	0.949	0.034	0.010		
26.498	0.487	0.014	0.006	22.0	6.1	57.372	4.146	0.029	0.082	81.0	2.7
26.669	0.217	0.010	0.004			59.066	0.589	0.028	0.004	107.2	19.4
27.575	0.165	0.021	0.002			60.045	0.285	0.017			
27.726	0.509	0.029	0.006	70.6	8.8	60.381	0.140	0.017	0.001		
28.355	0.570	0.009	0.008	44.7	3.7	61.258	1.672	0.044	0.017	74.7	9.6
28.903	0.467	0.009	0.006	48.6	4.7	61.613	0.434	0.025	0.004		
29.504	0.701	0.009	0.009	44.6	3.2	62.549	0.222	0.016	0.001		
29.956	0.050					63.507	0.199	0.018	0.001		
30.822	0.150	0.010	0.002			64.039	4.042	0.049	0.074	47.1	4.6

Table I
(continued)

E (eV)	$2g\Gamma_n$ (meV)	$\Delta(2g\Gamma_n)_s$ (meV)	$\Delta(2g\Gamma_n)_t$ (meV)	Γ_γ (meV)	$\Delta\Gamma_\gamma$ (meV)	E (eV)	$2g\Gamma_n$ (meV)	$\Delta(2g\Gamma_n)_s$ (meV)	$\Delta(2g\Gamma_n)_t$ (meV)	Γ_γ (meV)	$\Delta\Gamma_\gamma$ (meV)
64.539	1.954	0.052	0.025	38.3	9.2	106.396	3.352	0.180	0.054		
65.164	5.187	0.048	0.109	49.7	3.7	107.615	1.925	0.038	0.019		
65.733	1.090	0.046	0.010	18.8	14.0	109.824	3.256	0.144	0.042		
66.314	1.036	0.052	0.010	75.2	19.6	110.093	3.337	0.144	0.043		
66.874	2.105	0.044	0.025	71.9	8.1	111.170	0.374	0.059	0.003		
68.525	0.431	0.019	0.003			111.627	5.200	0.102	0.068	94.3	10.4
69.585	1.116	0.051	0.013			112.752	0.414	0.042	0.003		
69.824	2.661	0.053	0.040			113.280	0.300				
71.253	0.583	0.085	0.006			113.907	1.741	0.078	0.014	77.6	23.0
71.463	1.109	0.079	0.011			115.084	1.800	0.081	0.014	79.3	23.8
71.841	1.034	0.025	0.010			115.777	0.701	0.049	0.004		
72.276	0.226	0.021	0.001			116.396	2.623	0.081	0.023	42.0	15.6
74.969	0.481	0.020	0.004			117.656	0.030				
75.715	0.378	0.034	0.003			118.522	0.806	0.046	0.005		
75.943	0.515	0.027	0.003			119.823	2.237	0.131	0.022		
76.779	0.109					120.123	1.930	0.131	0.026		
78.191	1.486	0.099	0.015	10.3	17.4	121.982	3.216	0.138	0.033	36.9	19.0
78.551	1.179	0.105	0.011	60.8	26.0	122.662	3.893	0.222	0.040	64.2	27.6
79.555	0.730	0.023	0.005			123.283	3.534	0.146	0.035	56.3	20.5
80.050	0.546	0.029	0.004			124.946	1.640	0.054	0.013		
80.393	0.588	0.029	0.004			125.819	1.035	0.055	0.007		
81.077	0.106	0.039				126.441	2.035	0.057	0.017		
81.458	1.042	0.081	0.008	104.6	35.0	127.415	0.250				
82.089	1.454	0.054	0.015	26.7	14.0	127.994	1.688	0.056	0.013		
82.900	0.439	0.024	0.003			129.677	0.225		0.002		
83.370	0.431	0.024	0.003			130.720	1.358	0.072	0.009		
84.006	1.456	0.027	0.015	38.1	8.7	131.319	3.121	0.132	0.032	56.0	23.2
84.685	2.141	0.044	0.022			132.180	0.875	0.062	0.006		
86.610	0.225	0.025	0.001			132.754	1.180	0.059	0.008		
87.481	0.126	0.029				133.657	1.784	0.100	0.014	52.1	30.5
87.984	3.918	0.053	0.055	70.7	6.3	134.867	8.015	0.317	0.104		
89.297	0.332	0.041	0.002			135.449	4.131	0.348	0.042		
89.602	2.364	0.093	0.024	86.7	16.1	136.435	5.757	0.145	0.068	45.7	14.1
93.412	6.296	0.055	0.115	53.7	4.0	137.103	1.294	0.077	0.009		
94.610	0.754	0.030	0.006			137.613	1.628	0.064	0.012		
95.285	0.360	0.035	0.003			138.774	3.886	0.108	0.040	40.6	15.4
95.686	2.863	0.041	0.034			139.963	1.253	0.071	0.008		
96.100	2.906	0.048	0.037			140.498	2.436	0.073	0.021		
96.460	2.834	0.052	0.035			141.310	4.229	0.108	0.055		
97.423	0.277	0.030	0.001			141.520	3.256	0.106	0.039		
98.356	0.265	0.030	0.001			143.036	0.331	0.066	0.002		
100.156	1.075	0.033	0.009			144.869	1.421	0.068	0.010		
101.598	2.825	0.058	0.028	51.1	10.0	145.438	0.350				
102.555	0.248	0.035	0.001			146.436	1.739	0.070	0.012		
103.203	6.980	0.063	0.120	40.2	4.5	148.031	12.302	0.138	0.198		
104.788	2.196	0.059	0.022	40.2	12.8	149.141	3.926	0.076	0.039		
106.148	6.824	0.185	0.136								

Table II

Energy limits (eV)	Channel length for time-of-flight sector	- Accelerator pulse width: 100 ns
0.8 - 3.8	800	- Repetition rate - 500 Hz
3.8 - 9.7	400	
9.7 - 23.6	200	- Flight path length: 13 945 m
23.6 - 86.7	100	
86.7 - 152	50	- Accumulation time: 200 h.

Table III

E (eV)	Γ_f (meV)	E (eV)	Γ_f (meV)	E (eV)	Γ_f (meV)
1.28	0.37	10.12	0.16	24.19	0.14
1.93	0.08	10.40	0.06	25.63	0.29
2.37	0.18	10.99	0.13	26.50	0.05
2.60	0.17	12.88	0.06	26.67	0.19
3.97	0.16	14.68	0.27	28.36	0.16
4.97	0.44	15.69	0.10	28.90	0.16
5.42	0.63	16.39	0.11	29.50	0.10
6.12	0.42	16.85	0.32	31.25	0.22
6.74	0.22	17.73	0.30	32.03	0.28
7.66	0.10	19.44	0.03	36.98	0.51
8.17	0.12	21.74	0.27	38.37	0.30
9.11	0.18	23.08	0.27	39.62	0.23
9.85	0.95	23.34	0.17		

Table IV

E (eV)	Γ_f (meV)	E (eV)	Γ_f (meV)	E (eV)	Γ_f (meV)
22.75	0.58	30.82	1.20	40.07	0.79
23.08	0.77	31.02	0.51	40.41	0.34
23.34	0.31	31.25	0.57	43.29	0.35
24.19	0.48	32.03	0.56	43.57	0.49
25.63	0.82	34.03	0.22	46.07	0.27
26.50	0.47	34.46	0.74	46.57	0.28
26.67	0.48	34.93	0.41	47.54	0.25
27.57	2.54	35.49	0.36	48.76	0.49
27.73	0.44	36.25	0.57	49.33	0.54
28.36	0.55	36.99	0.66	50.28	0.37
28.90	0.36	38.37	0.53	50.85	0.47
29.50	0.45	39.62	0.56	51.98	0.38